Check for updates

Direct synthesis of poly(benzoxazine imide) from an *ortho*-benzoxazine: its thermal conversion to highly cross-linked polybenzoxazole and blending with poly(4-vinylphenol)†

Ahmed F. M. El-Mahdy[a,b] and Shiao-Wei Kuo [ID] *[a]

This paper describes a facile one-pot synthesis of a poly(benzoxazine imide), NDOPoda Bz, through the reaction of a difunctional naphthalene dianhydride *ortho*-phenol (ND-*ortho*-phenol), paraformaldehyde, and 4,4′-oxydianiline in 1,4-dioxane, without the need for either the preparation of an amino-functionalized benzoxazine or subsequent thermal treatment. This new poly(benzoxazine imide) underwent cross-linking polymerization to form a highly cross-linked poly(benzoxazine imide), which, with additional thermal treatment, was converted to highly cross-linked polybenzoxazoles. A model monomer (NDOPa Bz) was also synthesized based on the reaction of ND-*ortho*-phenol with paraformaldehyde and aniline. Moreover, we investigated the blending of NDOPoda Bz with a poly(4-vinylphenol) (PVPh) homopolymer at various weight ratios to form miscible blend systems. Fourier transform infrared spectroscopy, differential scanning calorimetry (DSC), and thermogravimetric analysis (TGA) revealed the thermal stability and thermal curing behavior of these blends, which were miscible because of strong hydrogen bonds between the C═O groups of PNDOPoda BZ and the OH groups of PVPh. The DSC and TGA data suggested that these hydrogen bonds enhanced the glass transition temperatures, thermal stability, and char yields of the blends. In addition, this approach decreased the temperature for ring opening of the benzoxazine, accelerated the rate of benzoxazole ring formation of NDOPda Bz at a lower temperature, and improved the thermal stability of the formed polybenzoxazoles.

Introduction

Benzoxazines are heterocyclic monomers that can be synthesized through Mannich condensations of primary aliphatic or aromatic amines, paraformaldehyde, and phenolic derivatives.[1–3] The wide variety of possible starting amines and phenols offers a high degree of flexibility in the molecular design of benzoxazine monomers.[4,5] Benzoxazine monomers can undergo self-cross linking polymerization through thermal ring-opening reactions, without the release of byproducts, and can be converted into thermosetting polybenzoxazines featuring three-dimensional network structures.[6,7] They have attracted much attention in academic and industrial fields because of the high flexibility of their molecular design and their excellent mechanical and physical properties. The features that make polybenzoxazines most attractive for use in many applications are their high glass transition temperatures (T_g), excellent mechanical and thermal properties, low dielectric constants, low moisture absorption, high dimensional stability, and low surface free energies.[8–16] Further tailoring of the physical properties of polybenzoxazines can be performed through structural modification or blending. In the former method, the introduction of inorganic (*e.g.*, carbon nanotubes,[17–19] clays,[20,21] polyhedral oligomeric silsesquioxanes)[22–24] or organic (*e.g.*, propargyl ethers, pyrenes, nitriles, methacrylols)[17,25–27] materials can improve the mechanical and thermal properties of polybenzoxazines through the formation of covalent cross-linked networks. In the latter, the thermal properties of polybenzoxazines can be modified through blending such polymers as poly(*N*-vinyl-2-pyrrolidone),[28] epoxy, and polyurethane resin.[29]

Aromatic polyimides are heterocyclic polymers that contain rigid cyclic imide functional groups in their main polymer backbone.[30,31] The family of polyimides has become more important in the past two decades because of their high glass transition temperatures and excellent balance of thermal and mechanical properties, making them useful materials for engineering applications.[32,33] The most commonly used poly-

[a]Department of Materials and Optoelectronic Science, National Sun Yat-Sen University, Kaohsiung 80424, Taiwan. E-mail: kuosw@faculty.nsysu.edu.tw
*[b]Chemistry Department, Faculty of Science, Assiut University, Assiut 71516, Egypt*
†Electronic supplementary information (ESI) available. See DOI: 10.1039/c8py00087e

imide is the polyether-imide (Kapton polyimide), which is synthesized through the reaction of pyromellitic anhydride with 4,4′-oxydianiline (ODA) in dimethylacetamide.[34] Nevertheless, these types of polymers, particularly those with *para*-substituted rings, typically exhibit limited solubility in organic solvents and poor process ability. Therefore, many efforts are being made to modify the chemical structures of polyimides, with the goals of lowering their glass transition temperatures to a range that would facilitate their processing in the melt and improving their solubilities in organic solvents.

Recently, a new class of highly stable polybenzoxazines has been developed, formed through thermal conversions of *ortho*-functional benzoxazines.[35–37] Compared with ordinary polybenzoxazines formed from *para*-functional benzoxazines, the *ortho*-functional polybenzoxazines exhibit several attractive features, including higher values of T_g and higher thermal stability.[38] A few other reports have appeared describing the synthesis of *ortho*-functional polybenzoxazines containing other organic groups, including amic acid, amide, imide, and amide–imide units.[39–42] As an example, the synthesis of functional *othro*-amide–imide benzoxazine polymer has been reported through the reaction of functional amide–imide *ortho*-phenol (**A**) with 4,4′-diaminodiphenylmethane (**B**) and paraformaldehyde in xylenes (Fig. S1†).[41] In addition, Wang *et al.* described the addition of *ortho*-imide moieties as end groups of benzoxazine polymer by the reaction of bisphenol-A (**C**) with 4,4′-diaminodiphenylmethane (**B**) and *o*-hydroxy phenylndimide in xylenes (Fig. S1†).[42] The resulting polybenzoxazines typically display high thermal stability, outstanding

flexibility in the molecular design, and cost-effectiveness. Furthermore, the incorporation of benzoxazines into polyimides can improve their dimensional stability, glass transition temperatures, contact angles, and thermal stability. As displayed in Fig. S2,† the only reported methods for introducing benzoxazines into polyimides are the reactions of primary amine-functionalized benzoxazines (**A**, **B**) with dianhydrides (**C**, **D**, **E**) at a molar ratio of 1 : 1 in dimethylacetamide at room temperature to produce poly(benzoxazine amic acid)s, which, under further thermal treatment, are converted to poly(benzoxazine imide) thermosets through thermal imidization of amic acid.[39,43]

In this paper, we present a novel class of ultrahigh-performance cross-linked poly(benzoxazine imide) thermosets prepared through a one-pot Mannich reaction of 2,7-bis(2-hydroxyphenyl)isoindolo[5,6-*f*]isoindole-1,3,6,8(2*H*,7*H*)-tetraone (ND-*ortho*-phenol), paraformaldehyde, and ODA (Scheme 1). Here, the incorporation of the smart *ortho*-phenol benzoxazine into the polyimide was performed in one step without the need to prepare an amine-functionalized benzoxazine or to perform further thermal treatment, as has been required previously.[39,43] The resulting poly(benzoxazine imide) could be further treated thermally to produce highly cross-linked poly(benzoxazine imide), which, with additional thermal treatment, could be converted into highly cross-linked polybenzoxazole. In addition, to improve the thermal properties of the resulting poly(benzoxazine imide) thermoset, we blended this polymer with homopolymeric poly(4-vinylphenol) (PVPh) to form miscible PNDOPoda Bz/PVPh blends. We have used
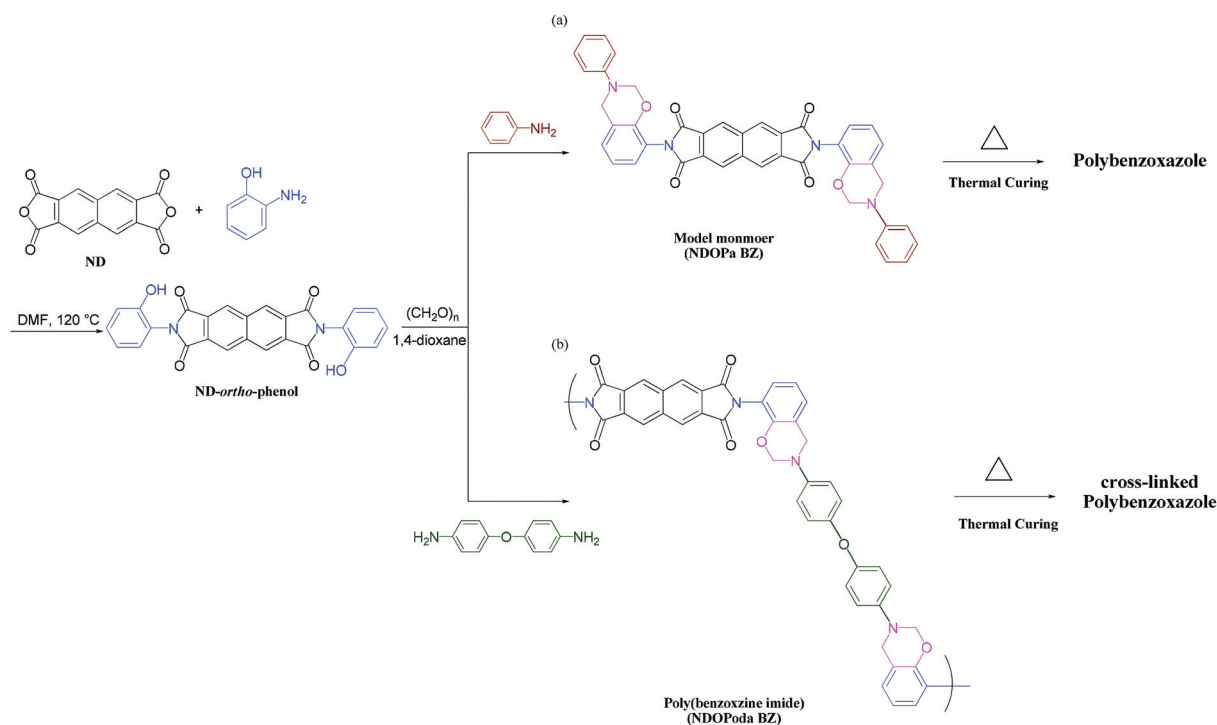
Scheme 1 Synthesis of (a) NDOPoa Bz monomer and (b) poly(benzoxazine imide) (NDOPoda BZ) polymer from ND–*ortho*–phenol, and their products of thermal curing.

Fourier transform infrared (FTIR) spectroscopy, differential scanning calorimetry (DSC), and thermogravimetric analysis (TGA) to study the thermal stability and thermal curing behavior of these poly(benzoxazine imide) and the hydrogen bonding between the poly(benzoxazine imide) and PVPh.

Experimental section

Materials

2.3,6,7-Naphthalenetetracarboxylic dianhydride (NTCDA, 97%) and *o*-aminophenol (99%) were used as received from Alfa Aesar. Paraformaldehyde (96%) and aniline (99.8%) were purchased from Acros. ODA (97%) and PVPh (M_w = *ca.* 11 000 g mol^{-1}) were obtained from Sigma–Aldrich. *N,N*-Dimethylformamide (DMF), methanol, 1,4-dioxane, and ethyl acetate were obtained from Acros and used as received.

Characterization

FTIR spectra of the synthesized compounds and polymers were measured using a Bruker Tensor 27 FTIR spectrophotometer and the conventional KBr plate method; 32 scans were collected at a resolution of 4 cm^{-1}. Proton and carbon nuclear magnetic resonance (^{1}H-NMR and ^{13}C-NMR) spectra were recorded using an INOVA 500 instrument with DMSO-d_6 as the solvent and tetramethylsilane (TMS) as the external standard. Chemical shifts were given in parts per million (ppm). Dynamic curing kinetics were examined using a TA Instruments Q-20 differential scanning calorimeter. All samples were placed in hermetic aluminum pans with lids and heated from 25 to 350 °C at a heating rate of 20 °C min^{-1} under a N$_2$ flow rate of 50 mL min^{-1}. TGA of the prepared samples was performed using a TA Q-50 analyzer under a N$_2$ atmosphere. The samples were sealed in a Pt cell and heated from 30 to 800 °C at a heating rate of 20 °C min^{-1} under a N$_2$ atmosphere (flow rate: 50 mL min^{-1}). Dynamic mechanical analysis (DMA) was performed on a PerkinElmer instrument model DMA 8000 apparatus over a temperature range from 30 °C to 400 °C at a heating rate of 5 °C min^{-1}. The sample was sandwiched between to Al sheets using single cantilever bending mode. The molecular distribution and molecular weight of the NDOPoda Bz polymer were measured through gel permeation chromatography (GPC) using a Waters 510 high performance liquid chromatography (HPLC) system equipped with a 410 differential refractometer and ultrastyragel columns (500, 580, and 10 Å) connected in series, with DMF as the eluent (flow rate: 0.4 mL min^{-1}).

2,7-Bis(2-hydroxyphenyl)isoindolo[5,6-*f*]isoindole-1,3,6,8 (2*H*,7*H*)-tetraone (ND-*ortho*-phenol)

2,3,6,7-Naphthalenetetracarboxylic dianhydride (1.00 g, 3.72 mmol), *o*-aminophenol (0.814 g, 7.46 mmol), and dry DMF (30 mL) were placed in a 100 mL two-neck round-bottom flask equipped with a stirrer bar. The mixture was stirred at room temperature for 2 h and then heated under reflux for 7 h. After cooling, the mixture was poured into ice-water

(200 mL) to give a yellow precipitate. The product was dried at 70 °C under vacuum overnight to obtain a yellow powder [yield: 94%; TLC: R_f = 0.15 (THF/hexane, 3 : 4)]. FTIR (KBr, cm^{-1}): 3428 (OH stretching), 1709 (imide C=O), 1662 (imide C=O), 1356 (C–N stretching), 763 (imide C=O bending), 753 (imide C=O bending). ^{1}H-NMR (500 MHz, DMSO-d_6): δ = 9.74 (s, 1H, OH), 8.73 (s, 4H, aromatic CH of naphthalene ring), 7.33 (d, 4H, aromatic CH), 7.02–6.96 (m, 4H, aromatic CH). ^{13}C-NMR (125 MHz, DMSO-d_6): δ = 163.15 (C=O), 153.96 (aromatic C–OH), 131.01–117.20 (aromatic C and CH).

2,7-Bis(3-phenyl-3,4-dihydro-2*H*-benzo[*e*][1,3]oxazin-8-yl) isoind-olo[5,6-*f*]isoindole-1,3,6,8 (2*H*,7*H*)-tetraone (NDOPa Bz)

A solution of ND-*ortho*-phenol (1.00 g, 2.22 mmol) in 1,4-dioxane (10 mL) was added dropwise to a stirred solution of aniline (0.420 g, 4.44 mmol) and paraformaldehyde (0.400 g, 13.3 mmol) in 1,4-dioxane (30 mL) in a 100 mL two-neck round-bottom flask cooled in an ice bath. The mixture was stirred at 110 °C for 20 h and then cooled to room temperature. The mixture was concentrated under vacuum and then added to cold water (100 mL) to precipitate a powder, which was filtered off and dissolved in ethyl acetate (100 mL). The organic phase was washed three times with 2 N NaOH and then with water to eliminate any residual staring materials. The organic phase was dried (anhydrous MgSO$_4$) for 2 h and gravity filtered. Evaporation of the solvent under vacuum gave a gray-white product [yield: 75%; TLC: R_f = 0.5 (THF/hexane, 3 : 4)]. FTIR (KBr, cm^{-1}): 1714 (imide C=O), 1674 (imide C=O), 1504 (vibration of trisubstituted benzene ring), 1350 (CH$_2$ wagging), 1246 (asymmetric COC stretching), 925 (oxazine ring), 767 (imide C=O bending), 749 (imide C=O bending). ^{1}H-NMR (500 MHz, DMSO-d_6): δ = 8.72 (s, 4H, aromatic CH of naphthalene ring), 7.30–6.88 (m, 16H, aromatic CH), 5.41 (s, 4H, OCH$_2$N), 4.76 (s, 4H, ArCH$_2$N). ^{13}C-NMR (125 MHz, DMSO-d_6): δ = 162.69 (C=O), 148.86 (aromatic C–O–CH$_2$ of benzoxazine ring), 148.13 (aromatic C–N), 129.63–112.73 (aromatic C and CH), 79.81 (OCH$_2$N), 67.58 (ArCH$_2$N).

Poly(2-(3-(4-(4-(2*H*-benzo[*e*][1,3]oxazin-3(4*H*)-yl)phenoxy) phenyl)-3,4-dihydro-2*H*-benzo [*e*][1,3]oxazin-8-yl)isoindolo [5,6-*f*]isoindole-1,3,6,8-(2*H*,7*H*)-tetraone) (NDOPoda Bz)

A solution of ND-*ortho*-phenol (1.00 g, 2.22 mmol) in 1,4-dioxane (10 mL) was added portion wise to a stirred solution of ODA (0.440 g, 4.44 mmol) and paraformaldehyde (0.4 g, 13.32 mmol) in 1,4-dioxane (30 mL) and DMF (10 mL) in a 100 mL two-neck round-bottom flask cooled in an ice bath. The mixture was stirred at 110 °C for 24 h and then cooled to room temperature. The mixture was filtered while hot and then the filtrate was poured into cold methanol (100 mL) to precipitate a powder, which was isolated through filtration and washed with methanol. The product was dried at 70 °C under vacuum overnight to obtain a white-gray powder (yield: 76%). FTIR (KBr, cm^{-1}): 1718 (imide C=O), 1679 (imide C=O), 1501 (vibration of trisubstituted benzene ring), 1348 (CH$_2$ wagging), 1251 (asymmetric COC stretching), 925 (oxazine ring), 767

(imide C=O bending), 748 (imide C=O bending). ^{1}H-NMR (500 MHz, DMSO-d_6): δ = 9.72 (OH), 8.72–8.67 (aromatic CH of naphthalene ring), 7.27–7.00 (aromatic CH), 5.34 (OCH$_2$N), 4.71 (ArCH$_2$N). ^{13}C-NMR (125 MHz, DMSO-d_6): δ = 162.84 (C=O), 151.19 (aromatic C–O–CH$_2$ of benzoxazine ring), 150.41 (aromatic C–N), 131.39–117.09 (aromatic C and CH), 80.14 (OCH$_2$N), 67.71 (ArCH$_2$N).

Blends of NDOPoda Bz and PVPh

Mixtures of NDOPoda Bz and PVPh were prepared by dissolving desired weight percentages of PVPh (20–80%) with NDOPoda Bz in DMF (5 mL) in 20 mL sample vials equipped with stirrer bars. The solutions were ultrasonicated for 15 min and then stirred at room temperature for 72 h. The solvent was then evaporated under high vacuum at 70 °C for 72 h.

Results and discussion

Preparation of NDOPa Bz monomer and poly(benzoxazine imide) (NDOPda Bz)

Our objective for this study was to incorporate a smart *ortho*-phenol benzoxazine into a polyimide through a one-pot reaction. First, we synthesized the difunctional naphthalene dianhydride *ortho*-phenol (ND-*ortho*-phenol) through the reaction of naphthalene tetracarboxylic dianhydride (ND) and *o*-aminophenol in DMF, and then used it in the preparation of the model naphthalene dianhydride *ortho*-phenol/aniline benzoxazine monomer (NDOPa Bz) and poly(benzoxazine imide) (NDOPda Bz), as displayed in Scheme 1. We select naphthalene tetracarboxylic dianhydride (ND) instead of pyromellitic dianhydride (PD) due to the rigid structure of ND. It has been reported that the molecular structure of ND has a rigid structure compared with that of PD. The rigid structure of ND decreased the ring-opening of dianhydride ring during its reaction with amines. In addition, the formed polyimides possess a massive number of geometric plane structures of ND units, which improved the heat resistance (*e.g.* glass transition temperature) and also showed low water adsorption compared with polyimides formed from PD.[44] The model benzoxazine monomer (NDOPa Bz) was prepared through a Mannich reaction of ND-*ortho*-phenol, paraformaldehyde, and aniline in 1,4-dioxane at 90 °C for 24 h, while poly(benzoxazine imide) (NDOPda Bz) was prepared through a Mannich reaction of ND-*ortho*-phenol, paraformaldehyde, and ODA in 1,4-dioxane at 90 °C for 24 h.

Previously, Huang *et al.*[45] reported that the difunctional *para*-imide benzoxazine could be prepared over a much longer time (72 h) in 1,4-dioxane under reflux. While, Ishida *et al.*[46] reported the synthesis of functional *ortho*-imide benzoxazines with *ca.* 87–96% yield over a short time (6–12 h) in xylenes, but with a much higher temperature 120 °C. In our case, however, the difunctional *ortho*-imide benzoxazine monomer NDOPa Bz and the poly(benzoxazine imide) NDOPda Bz were obtained within 24 h at 90 °C, with transparent solutions usually formed, leading to high yields. We suspect that the high yields
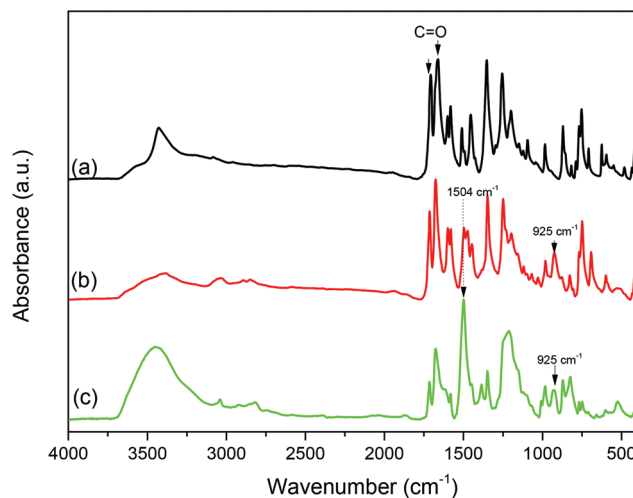

Fig. 1 FTIR spectra of (a) ND-*ortho*-phenol, (b) NDOPa Bz, and (c) NDOPoda Bz, recorded at room temperature.

of NDOPa Bz and NDOPda Bz arose from the hydrogen bond formed between the phenolic (OH) group and one of the carbonyl (C=O) groups, thereby decreasing the polarity of ND-*ortho*-phenol and increasing its solubility in 1,4-dioxane, an aprotic solvent. The structures of difunctional *ortho*-imide phenol (ND-*ortho*-phenol), benzoxazine monomer (NDOPa Bz) and poly(benzoxazine imide) (NDOPoda Bz) were confirmed through FTIR, ^{1}H-NMR, and ^{13}C-NMR spectroscopic analyses. Fig. 1 presents the ambient-temperature FTIR spectra of ND-*ortho*-phenol, NDOPa Bz, and NDOPoda Bz. The spectrum of ND-*ortho*-phenol features [Fig. 1(a)] a broad signal at 3428 cm^{-1} for the stretching of the OH group and two sharp signals at 1709 and 1662 cm^{-1} for the stretching of the imide C=O groups. The signal at 1356 cm^{-1} was due to the axial stretching of the C–N bond. The spectra of NDOPa Bz and NDOPda Bz [Fig. 1(b) and (c)] are characterized by signals for the imide C=O groups at 1714/1674 and 1718/1679 cm^{-1}, respectively. We confirmed the benzoxazine structures by the appearance of signals for asymmetric trisubstituted benzene and oxazine rings at 1504 and 925 cm^{-1} for NDOPa Bz and at 1501 and 925 cm^{-1} for NDOPoda Bz. Furthermore, the presence of benzoxazine rings was indicated by signals representing C–O–C stretching at 1246 and 1251 cm^{-1} for NDOPa Bz and NDOPda Bz, respectively.

Fig. 2(a) presents the ^{1}H-NMR spectrum of ND-*ortho*-phenol. The characteristic signals of the OH, naphthalene CH, and other aromatic CH units appear at 9.74, 8.73, and 7.33–6.96 ppm, respectively. The benzoxazine rings of NDOPa Bz and NDOPda Bz are characterized by the appearance of two bands at 5.41 (OCH$_2$N)/4.76 (ArCH$_2$N) ppm and 5.34 (OCH$_2$N)/4.71 (ArCH$_2$N) ppm, respectively; no signal for a NCH$_2$-Ar unit was present close to 4.00 ppm, indicating that ring opening of the benzoxazine moiety had not occurred. The integration ratio for the signals at 5.41 and 4.76 ppm was 1 : 1; for the signals at 5.34 and 4.71 ppm it was 1 : 1. Thus, our samples of
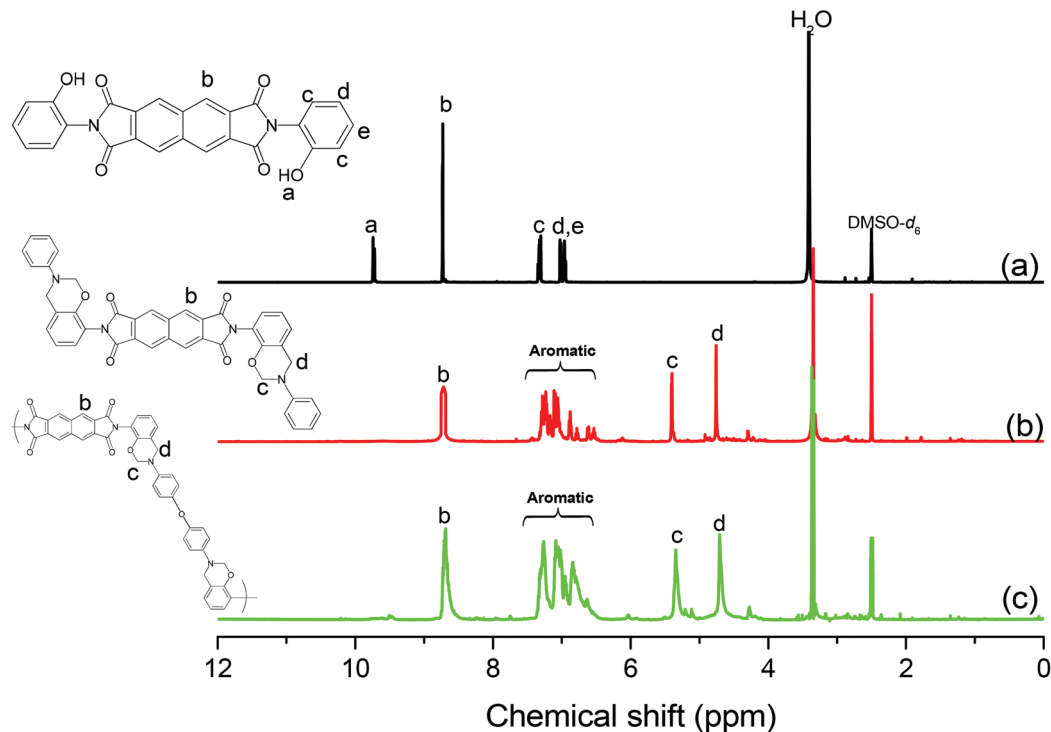
Fig. 2 ^{1}H-NMR spectra of (a) ND-*ortho*-phenol, (b) NDOPa Bz, and (c) NDOPoda Bz.

NDOPa Bz and NDOPoda Bz were highly pure. In addition, the phenolic OH was also observed for NDOPoda BZ is due to the chain end from ND-*ortho*-phenol unit. Moreover, the ^{1}H-NMR spectra confirmed the presence of imide rings, not amic acid units, from the appearance of symmetric signals for the aromatic CH units of the naphthalene rings at 8.72 and 8.72–8.67 ppm for NDOPa Bz and NDOPoda Bz, respectively [Fig. 2(b) and (c)].

^{13}C-NMR spectroscopic analysis confirmed the structure of ND-*ortho*-phenol and the formation of benzoxazine rings in NDOPa Bz and NDOPoda Bz. Fig. 3(a) presents the ^{13}C-NMR spectrum of ND-*ortho*-phenol: the characteristic signals for its C=O and C–OH groups appeared at 163.15 and 153.96 ppm, respectively. In the spectra of NDOPa Bz and NDOPoda Bz, the characteristic signals for the OCH$_2$N and ArCH$_2$N groups of the benzoxazine rings appeared at 79.81/67.58 and 80.14/67.71 ppm, respectively [Fig. 3(b) and (c)]. The signals for the symmetric C=O groups of the imide moieties appeared as singlets at 162.69 and 162.84 ppm for NDOPa Bz and NDOPoda Bz, respectively, confirming that the imide ring remained closed and had not been converted into the open-ring amic acid form. All of this information is consistent with the successful preparation of the target compounds and polymer. We used GPC to measure the molecular weight of the poly(benzoxazine imide) (NDOPoda Bz); its number-average molecular weight (M_n) was 14 800 g mol^{-1} and its weight-average molecular weight (M_w) was 16 300 g mol^{-1}, giving a polydispersity index (PDI) of 1.10.

Thermal polymerization of NDOPa Bz monomer and poly (benzoxazine imide) (NDOPoda Bz)

To examine the ring-opening polymerization of this new class of poly(benzoxazine imide) thermosets (NDOPoda Bz), we first used DSC and FITR spectroscopy to study the thermal polymerization behavior of the model NDOPa Bz monomer. Fig. 4(A) presents the DSC thermograms of the NDOPa Bz monomer after each curing stage, recorded at temperatures from 50 to 300 °C under a N$_2$ atmosphere at a heating rate of 20 °C min^{-1}. The DSC pattern of the uncured NDOPa Bz monomer featured an exothermic peak with a maximum temperature of 234 °C and a heat of polymerization of 122.6 J g^{-1}. The enthalpies of the exotherms of NDOPa Bz decreased upon increasing the curing temperature. The exothermic peak disappeared totally when applying curing temperatures above 180 °C, suggesting that the polymerization temperature of NDOPa Bz was greater than 180 °C. On the other hand, the values of T_g of the poly(NDOPa Bz) increased upon increasing the curing temperature: the values of T_g of NDOPa Bz were 145 and 188 °C when the thermal curing temperatures were 150 and 180 °C, respectively. Fig. 4(B) displays the FTIR spectra of the NDOPa Bz monomer and its polymeric products after each curing stage; we monitored the characteristic benzoxazine peak at 1252 (asymmetric C–O–C stretching) and 925 (oxazine ring) cm^{-1}. The intensities of these characteristic absorption peaks decreased progressively upon increasing the curing temperature from 150 to 180 °C, completely disappearing at temperatures above 180 °C, suggesting that a suitable tempera-
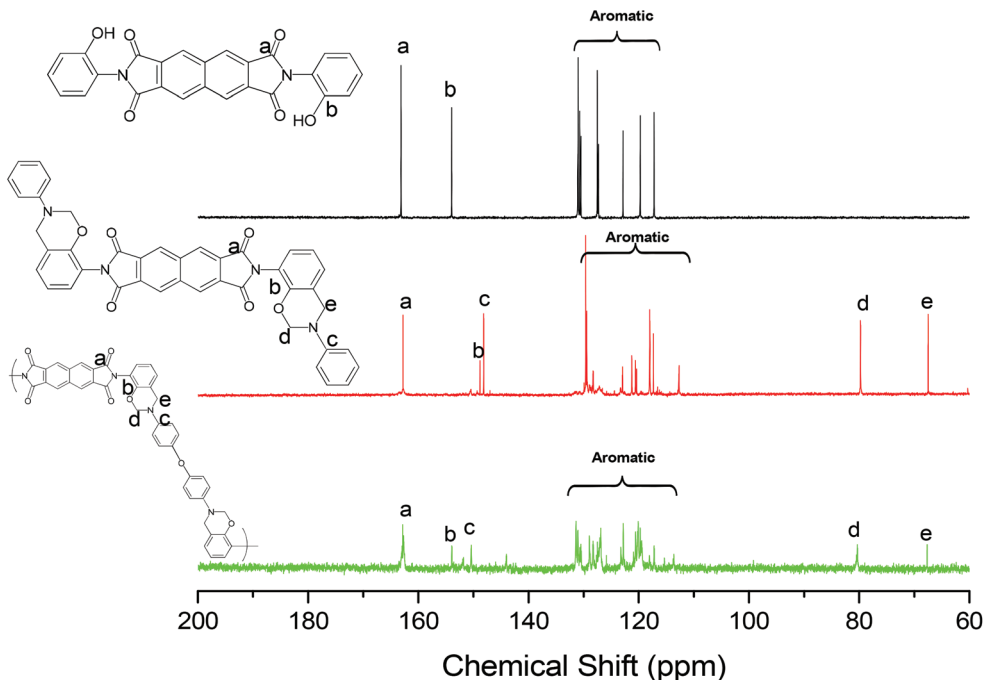
Fig. 3 ^{13}C-NMR spectra of (A) ND-*ortho*-phenol, (B) NDOPa Bz, and (C) NDOPda Bz.
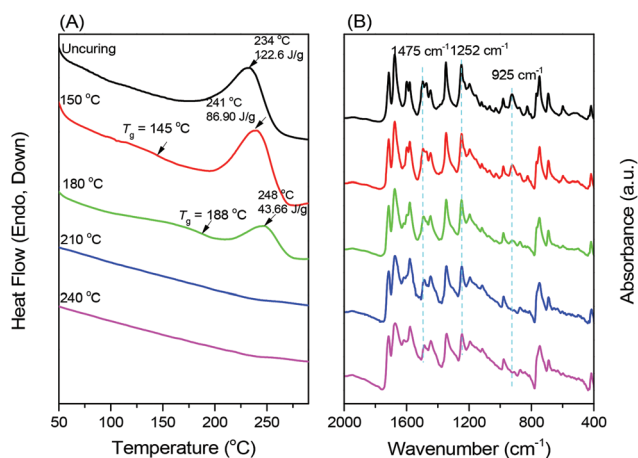

Fig. 4 (A) DSC thermograms and (B) FTIR spectra of NDOPa Bz after each heating stage.
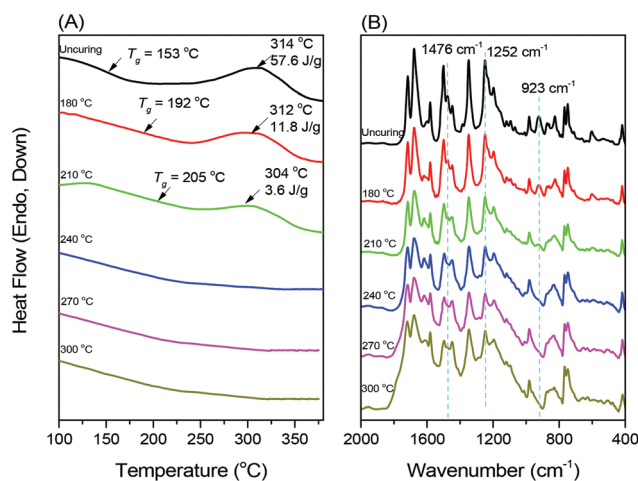

Fig. 5 (A) DSC thermograms and (B) FTIR spectra of NDOPoda Bz after each heating stage.

ture for the ring-opening polymerization of the NDOPa Bz monomer was a temperature higher than 180 °C. Thus, the FTIR spectral data were consistent with the DSC thermograms. Next, we used DSC and FTIR spectroscopy to study the thermal behavior of the poly(benzoxazine imide) thermoset (NDOPoda Bz). Fig. 5(A) displays the DSC traces for the cross-linking polymerization of NDOPoda Bz after each curing stage, recorded from 100 to 380 °C under a N_2 atmosphere at a heating rate of 20 °C min^{-1}. The thermogram of the uncured NDOPoda Bz gave a value of T_g of 153 °C and an exothermic peak with a maximum temperature of 314 °C and a heat of polymerization of 57.6 J g^{-1}. After thermal curing at 180 and

210 °C, the values of T_g of the cross-linked poly(NDOPda Bz) products increased to 192 and 205 °C, respectively, while the maxima of their exothermic peaks decreased to 312 and 304 °C, respectively, with reaction heats of 11.8 and 3.6 J g^{-1}, respectively. After thermal curing at 240 °C, the exothermic peak disappeared completely, indicating that suitable temperatures for ring-opening of the benzoxazine rings and for cross-linked polymerization were higher than 210 °C. Moreover, after curing at 270 and 300 °C, the exothermic peak remaining absent. The increase in the value of T_g upon increasing the curing temperature was due to the high crosslinking density
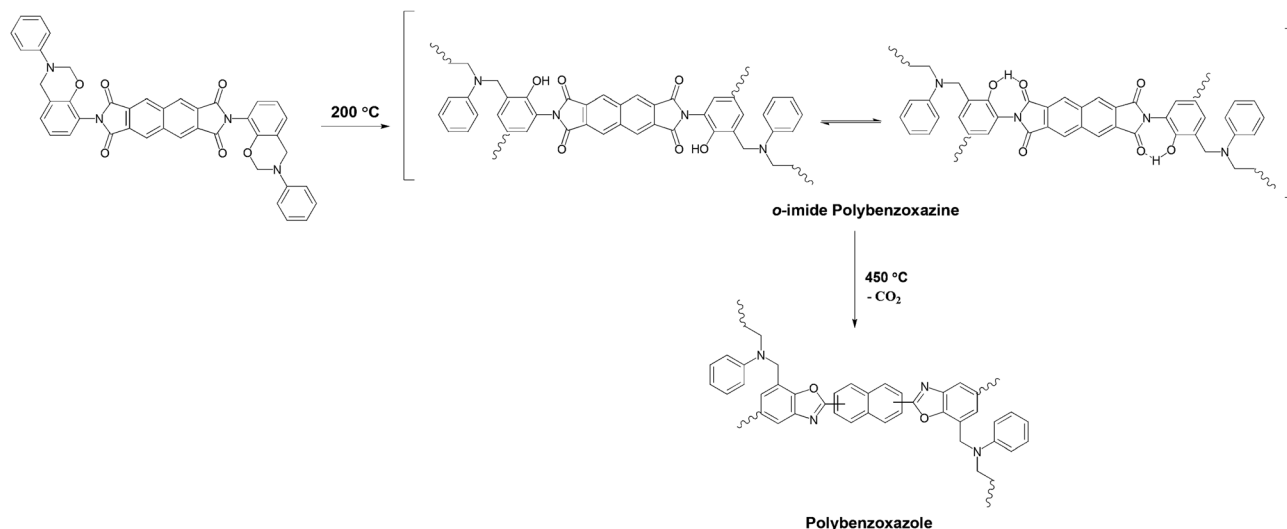
Scheme 2 Polymerization and thermal conversion behavior of NDOPa Bz monomer.

and the formation of a highly cross-linked thermoset. We also used FTIR spectroscopy to characterize the cross-linked structures formed after the curing of NDOPoda Bz at various heating stages. As displayed in Fig. 5(B), the intensities of the absorption signals at 925 and 1251 cm^{-1}, which represented the oxazine ring bending and asymmetric C–O–C stretching vibrations of the benzoxazine ring, decreased upon increasing the curing temperature from 180 to 210 °C. In contrast, the absorption band at 923 cm^{-1} disappeared completely when the curing temperature was between 240 and 300 °C. Thus, the DSC and FTIR spectral data were comparable, and confirmed that the benzoxazine rings in the poly(benzoxazine imide) (NDOPda Bz) could be opened thermally, without the use of catalysis, to form a highly cross-linked poly(benzoxazine imide) thermoset. In addition, Fig. S3† presents scale-expanded FTIR spectra [Fig. 4(B) and 5(B)] of NDOPa Bz and NDOPoda BZ after each heating stage. Again, we observed that the signals for the asymmetric and symmetric imide C=O stretching near 1715 and 1678 cm^{-1} broadened and a new absorption appeared near 1663 cm^{-1} as a result of intramolecular hydrogen bonding of the *ortho*-phenol and C=O units, as displayed in Scheme 2, upon increasing the curing temperature.

TGA of NDOPa Bz monomer and poly(benzoxazine imide) (NDOPoda Bz)

We used TGA and FTIR spectroscopy to investigate the thermal stabilities of the NDOPa Bz monomer and the poly(benzoxazine imide) (NDOPda Bz polymer) and the formation of polybenzoxazoles. Fig. 6 presents the TGA traces of the model NDOPa Bz monomer after curing at various temperatures, recorded at temperatures from 50 to 800 °C under a N$_2$ atmosphere at a heating rate of 20 °C min^{-1}. We used the 10% weight loss temperature (T_{d10}) as the standard. The values of T_{d10} and the char yields corresponding to the thermal
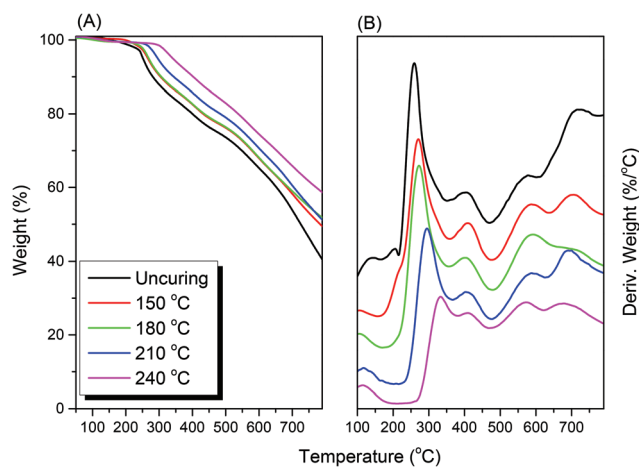
Fig. 6 TGA analyses of NDOPa Bz after each heating stage.

polymerization of NDOPa Bz both increased upon increasing the temperature of curing. The uncured NDOPa Bz monomer exhibited a value of T_{d10} of 279 °C and a char yield of 41%; after curing at 240 °C, these values were 400 °C and 60%, respectively [Fig. 6(A)]. On the other hand, the derivatives weight loss curves revealed a weight-loss stage in the range 250–350 °C [Fig. 6(B)]. This weight-loss in the range of 250–300 °C can be caused by the low heat of the polymerization of benzoxazines which making a few terminal groups in the formed *o*-imide polybenzoxazine are partially decomposed before its transformation into polybenzoxazole.[40] In addition, a weight loss stage in the range 350–450 °C was due to the release of CO$_2$ in the formation of polybenzoxazoles (Scheme 2). The degradation observed in the range 500–650 °C can presumably be attributed to decomposition of the oxazole rings or other groups. This suggestion of the formation of polybenzoxazole after further thermal treatment is consistent with

Ishida *et al.*'s suggestion.[39] It was reported that the *o*-imido polybenzoxazine (cross-linked polyimide, cPI) can undergo further cyclization to form polybenzoxazole after additional thermal treatment.

To further support the formation of polybenzoxazoles, we performed FTIR spectral analyses of NDOPa Bz samples after TGA from room temperature to 450 and 600 °C [Fig. S4(b) and S4(c)†]. The FTIR spectrum of the *o*-imide polybenzoxazines formed after thermal curing of NDOPa Bz at 210 °C was characterized by the appearance of two absorption bands at 1715 and 1678 cm^{-1}, attributed to asymmetric and symmetric imide C=O stretching [Fig. S4(a)†]. The FTIR spectra of NDOPa Bz after TGA heating from room temperature to 450 °C revealed the disappearance of the characteristic bands at 1715 and 1678 cm^{-1}, with a new band appearing for C=N stretching[38] of a benzoxazole at 1629 cm^{-1} [Fig. S4(b)†]. On the other hand, after TGA heating from room temperature to 600 °C, the absorption band of the benzoxazole at 1629 cm^{-1} remained, with its intensity much stronger than those of the other bands, suggesting that the degradation in the temperature range from 500 to 600 °C was attributable to decomposition of groups than the oxazole rings [Fig. S4(c)†]. The FTIR spectral data were comparable with the TGA data, suggesting that the thermal conversion of the *o*-imide polybenzoxazines into polybenzoxazoles was complete at a temperature below 450 °C and that the resulting polybenzoxazoles were thermally stable at temperatures of up to 600 °C.

Subsequently, we used TGA and FTIR spectroscopy to study the thermal stability of the poly(benzoxazine imide) (NDOPoda Bz polymer) and its thermal conversion into cross-linked polybenzoxazoles. Fig. 7 displays TGA traces of the NDOPda Bz polymer measured after each curing stage from 100 to 800 °C at a heating rate of 20 °C min^{-1}. In Fig. 7(A), we observed that the values of T_{d10} and the char yields, corresponding to the thermal reaction of NDOPoda Bz polymer, increased upon increasing the temperature of curing. The uncured NDOPoda Bz polymer exhibited a value of T_{d10} of 429 °C and a char yield

of 29%; after curing at 300 °C, the NDOPoda Bz polymer displayed a value of T_{d10} of 460 °C and a char yield of 33% [Fig. 7 (A)]. Furthermore, the derivative weight loss curves of the NDOPda Bz polymer and its curing products revealed a higher weight-loss stage in the range 550–700 °C, presumably due to thermal degradation of the oxazine rings or other groups [Fig. 7(B)]. The formation of cross-linked polybenzoxazines and cross-linked polybenzoxazoles was indicated by the appearance of low weight-loss stages in the ranges 300–400 and 400–500 °C, respectively.

The formation of the cross-linked poly(benzoxazine imide) and the cross-linked polybenzoxazole was also supported by measuring the FTIR spectra of the NDOPda Bz polymer after TGA treatment from room temperature to 500 and 650 °C. As displayed in Fig. S5(a),† the FTIR spectrum of the cross-linked poly(benzoxazine imide) formed after thermal curing of the NDOPda Bz polymer at 240 °C featured signals for asymmetric and symmetric imide C=O stretching at 1718 and 1679 cm^{-1}. On the other hand, a new strong absorption band appeared at 1629 cm^{-1}, representing C=N stretching of the benzoxazole, after TGA heating of the NDOPda Bz polymer from room temperature to 500 °C; meanwhile, the intensities of the characteristic bands at 1718 and 1679 cm^{-1} are decreased dramatically [Fig. S5(b)†]. After TGA heating of the NDOPoda Bz from room temperature to 650 °C, the intensity of the benzoxazole band at 1629 cm^{-1} had increased significantly, while the other two imide C=O bands at 1718 and 1679 cm^{-1} had disappeared completely [Fig. S5(c)†]. The FTIR spectral data suggested that the thermal conversion of the cross-linked poly(benzoxazine imide) into the cross-linked polybenzoxazole could be achieved at 500 °C and that the formed polybenzoxazole was thermally stable at temperatures up to 650 °C.

Dynamic mechanical analysis (DMA) NDOPa Bz monomer and poly(benzoxazine imide) (NDOPoda Bz) after thermal curing

The dynamic mechanical analysis (DMA) was used to investigate the glass transition temperature (T_g) for the *o*-imide polybenzoxazine and polybenzoxazole formed after thermal curing of the NDOPa Bz monomer at 210 °C and 450 °C and for the cross-linked poly(benzoxazine imide) and cross-linked polybenzoxazole formed after thermal curing of NDOPda Bz polymer at 240 °C and 500 °C. As shown in Fig. S6(a),† the *o*-imide polybenzoxazine of NDOPa Bz monomer exhibited a value of T_g from the loss tan δ peak of 355 °C. However, polybenzoxazole showed no value of T_g before 400 °C as shown in Fig. S6(b),† which indicated that this formed polybenzoxazole have massive thermal properties and can be used for various applications in very high temperature. We do not measure the value of T_g of polybenzoxazole at a higher temperature than 400 °C due to the thermal degradation of polybenzoxazole. On the same manner, the cross-linked poly(benzoxazine imide) formed from NDOPda Bz polymer showed a value of T_g of 385 °C (Fig. S7(a)†), was higher than that of *o*-imide polybenzoxazine of NDOPa Bz monomer, indicating its high cross-linked density when compared with that of *o*-imide polybenzoxazine. In addition, as shown in Fig. S7(b),† the cross-
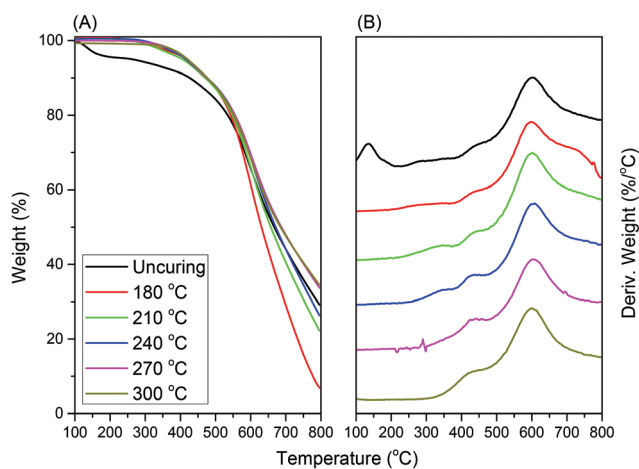

Fig. 7 TGA analyses of the NDOPda Bz polymer after each heating stage.

linked polybenzoxazole also showed no value of T_g before 400 °C. The values of T_g of *o*-imide polybenzoxazine of NDOPa Bz monomer and cross-linked poly(benzoxazine imide) from NDOPda Bz polymer in this study is higher than that of the *o*-imido polybenzoxazine (T_g = 308 °C) in the previous study.[39] All the DMA results indicated that the presence of much rigid naphthalene dianhydride moities in the main skeleton of polybenzoxazines, improved their thermal properties and produced polybenzoxazoles with much high T_g value which can be used for mechanical applications under very high temperatures.

Thermal properties of NDOPoda Bz/PVPh blends

To improve the thermal properties of our new poly(benzoxazine imide) thermoset, we investigated the ability of our NDOPoda Bz to interact with the phenol-containing PVPh through hydrogen bonding. Fig. 8(A) presents DSC thermograms of NDOPda Bz/PVPh blends containing various weight ratios of PVPh. The DSC profile of PVPh featured a value of T_g of 180 °C, while that of the pure NDOPoda Bz revealed a value of T_g of 153 °C and an exothermic peak having a maximum temperature of 314 °C and a reaction heat of 57.6 J g^{-1}. The maxima of the exothermic peaks of the NDOPoda Bz/PVPh blends decreased from 293 to 283 °C upon increasing the content of PVPh from 20 to 80%, indicating that hydrogen bonding between the phenolic OH groups of PVPh and one of the C=O groups of NDOPoda Bz accelerated the ring-opening reactions of the benzoxazine rings. In contrast, the values of T_g of the NDOPoda Bz/PVPh blends increased from 163 to 175 °C upon increasing the content of PVPh from 20 to 80%. The single values of T_g suggested that the PVPh was dispersed uniformly in the NDOPoda Bz matrix and stabilized through C=O···HO hydrogen bonding in the NDOPda Bz/PVPh blends. We also used FTIR spectroscopy as a tool to investigate the hydrogen bonds in the NDOPoda Bz/PVPh blends. Fig. 8(B)

displays FTIR spectra (1800–1600 cm^{-1} region) of the NDOPoda Bz/PVPh blends of various weight ratios, recorded at room temperature.

The spectrum of NDOPoda Bz features absorption bands at 1718 and 1678 cm^{-1} representing the imide C=O asymmetric and symmetric stretching modes, respectively;[47] the spectrum of the pure PVPh did not feature any characteristic absorption bands in the region from 1800 to 1600 cm^{-1}. In contrast, the hydrogen bonding of the C=O groups of the NDOPda in the NDOPda Bz/PVPh blends could be monitored by observing the shift in the signal for symmetric C=O stretching at 1678 cm^{-1}. The signal for the hydrogen-bonded C=O groups of NDOPoda shifted to lower wavenumber (1656 cm^{-1}) upon increasing the percentage of the PVPh homopolymer, suggesting strong hydrogen bonding between NDOPoda BZ and PVPh. Fig. 9(A) summarizes the results of curve fitting of the FTIR spectral signals of the NDOPoda Bz/PVPh blends, where these two peaks were fitted well by Gaussian functions. To determine the content of hydrogen-bonded C=O imide units of the NPOPoda BZ, we employed an absorptivity ratio α_{HB}/α_F of 1.3 for the C=O imide units. The fraction of hydrogen-bonded C=O imide units of the NPOPoda BZ increased upon increasing the content of PVPh [Fig. 9(B)]. We could use this information to determine the inter-association equilibrium constant (K_A) for the NPOPoda BZ/PVPh blends based on the Painter–Coleman association model. Accordingly, we obtained a value of K_A of 37 through least-squares fitting of the experimentally determined fraction of hydrogen-bonded C=O units, as also displayed in Fig. 9(B). Table S1† summarizes the thermodynamic parameters for the NPOPoda BZ/PVPh blends, where K_2 and K_B are the equilibrium constants for the PVPh self-association hydrogen-bonded dimer and multimer, respectively. The value of K_A of 37 is similar to that for typical OH···O=C inter-association hydrogen bonding in PMMA/ PVPh blend systems.[48]
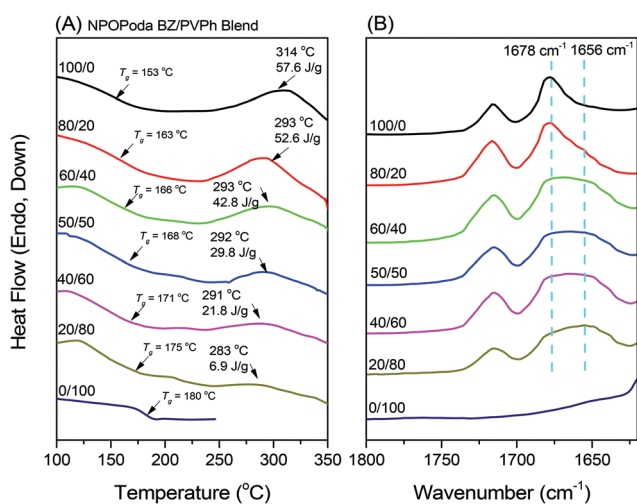

Fig. 8 (A) DSC traces and (B) FTIR spectra of NDOPoda Bz/PVPh blends of various ratios.
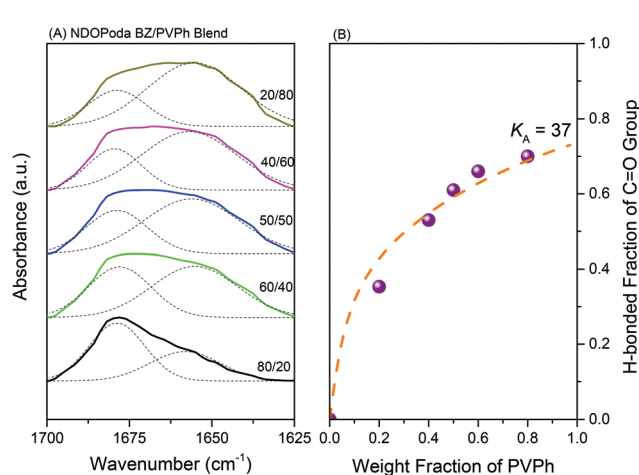

Fig. 9 (A) Curve fitting of the signals in the FTIR spectra of the NDOPoda Bz/PVPh blends. (B) Determining the value of K_A based on Painter–Coleman association model.
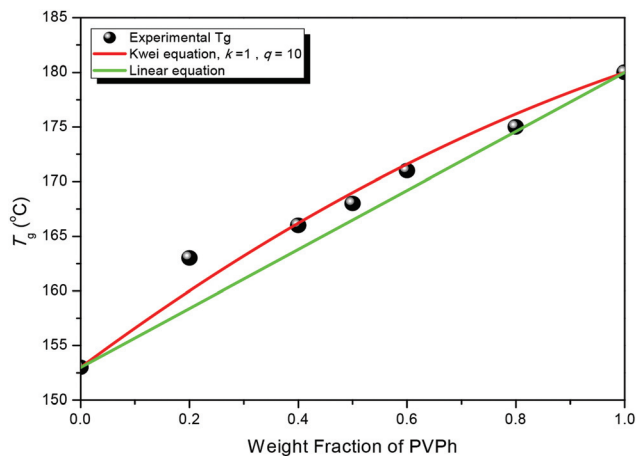
Fig. 10 Glass transition temperature–composition curves, based on the Kwei equation, for NDOPoda Bz/PVPh blends of various ratios.

Fig. 11 (A) FTIR spectra and (B) DSC traces of the NDOPda Bz/PVPh blend (50/50) after each heating stage.

Furthermore, we examined the glass transition behavior of the NDOPda Bz/PVPh miscible polymer blends containing various weight fractions of the PVPh segments (Fig. 10). The values of T_g revealed a large positive deviation from the linear rule, suggesting the presence of strong hydrogen bonding in this blend system. Generally, the relationship between the glass transition temperature and the composition of a NDOPoda Bz/PVPh miscible blend should follow the Kwei equation:[49]

$$T_g = \frac{W_1 T_{g1} + k W_2 T_{g2}}{W_1 + k W_2} + q W_1 W_2$$

where W_1 and W_2 are the weight fractions of NDOPoda Bz and PVPh, respectively; T_{g1} and T_{g2} are the corresponding glass transition temperatures of NDOPoda Bz and PVPh, respectively; and k and q are fitting constants. As displayed in Fig. 10, the values of k and q were determined, according to a non-linear least-square "best fit" approach, to be 1 and 10, suggesting the presence of intermolecular hydrogen bonding between NPOPoda BZ and PVPh, as confirmed through the FTIR spectroscopic analyses.

After confirming the presence of strong hydrogen bonding between the NDOPda Bz polymer and the homopolymeric PVPh, we used DSC and FTIR spectroscopy to investigate the thermal properties of the NDOPda Bz/PVPh blend at a weight ratio of 50 : 50 as a standard. Fig. 11(A) presents the DSC thermograms of the NDOPda Bz/PVPh (50 : 50) blend after each curing stage, recorded from 100 to 350 °C under a N$_2$ atmosphere. The DSC thermogram of the uncured blend featured a value of T_g of 168 °C and an exothermic peak with a heat of polymerization of 29.8 J g^{-1} and a maximum temperature of 292 °C. As the curing temperature increased to 180 and 210 °C, the values of T_g of the blend increased to 190 and 204 °C, respectively, with the minimum of the exothermic peak increasing to 293 and 309 °C, respectively, with reaction heats of 22.4 and 17.2 J g^{-1}, respectively. The exothermic peak of the blend disappeared after curing at 240 °C, indicating that
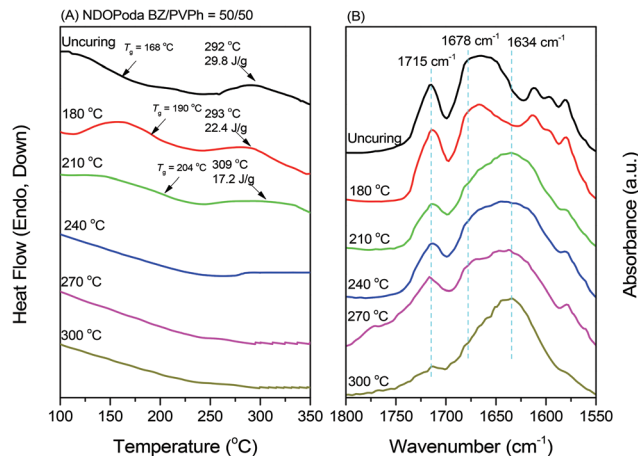
a suitable temperature for ring opening of the benzoxazine units in the blend was above 210 °C, leading to a highly cross-linked poly(NDOPda Bz/PVPh) product having a value of T_g of above 400 °C (from DMA). We also used FTIR spectroscopy to characterize the formation of the highly cross-linked poly(NDOPda Bz/PVPh) product after curing of the NDOPda Bz/PVPh (50 : 50) blend at various heating stages. As revealed in Fig. 11(B), the intensities of the characteristic absorption bands for the asymmetric C–O–C stretching and the oxazine ring bending vibrations of the benzoxazine at 1251 and 925 cm^{-1}, respectively, decreased gradually upon increasing the curing temperature from 180 to 210 °C, with the latter absorption band disappearing completely after curing at temperatures from 240 to 300 °C. The FTIR data are comparable with the DSC data. Most interestingly, upon increasing the curing temperature, the intensities of the absorption bands at 1715, 1678, and 1656 cm^{-1} (representing the imide asymmetric and symmetric C=O stretching modes and the hydrogen-bonded C=O groups, respectively) of the NDOPda all decreased, while a new absorption band appeared at 1634 cm^{-1}. We attribute this new absorption band to C=N stretching of the benzoxazole ring,[50] suggesting that the presence of PVPh accelerated the benzoxazole ring formation of NDOPda Bz at a lower temperature.

We used TGA to investigate the thermal stability of the NDOPoda Bz/PVPh (50 : 50) blend under a N$_2$ atmosphere. Fig. 12(A) reveals that the value of T_{d10} and char yield after thermal treatment of the NDOPoda Bz/PVPh (50 : 50) blend both increased upon increasing the temperature of curing. The uncured blend exhibited a value of T_{d10} of 330 °C and a char yield of 37%; after curing at 300 °C, these values were 461 °C and 52%, respectively. Fig. 12(B) presents the derivative weight loss curves of the NDOPda Bz/PVPh (50 : 50) blend and its curing products. The derivative loss curve of the uncured blend was characterized by three weight-loss stages: the first in the range 150–250 °C, due to the degradation of some terminal groups after ring-opening of the benzoxazine rings; the second
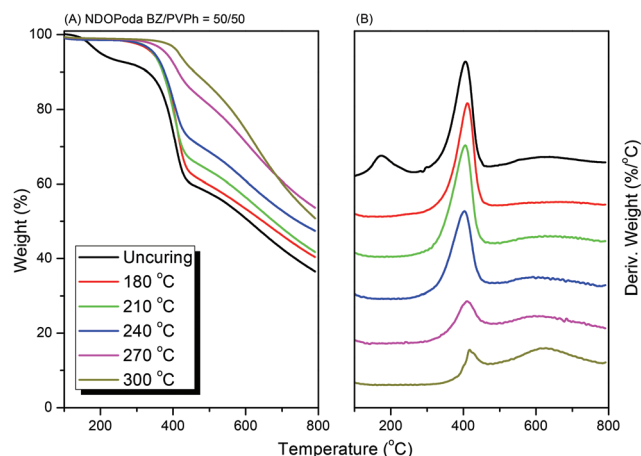
Fig. 12 TGA analyses of the NDOPda Bz/PVPh (50/50) blend after each heating stage.

in the range 300–450 °C, due to the formation of benzoxazoles and the degradation of PVPh; and the third in the range 500–700 °C, attributed to decomposition of the other groups. Moreover, the characteristic weight-loss stage of the ring-opening reaction disappeared after curing from 180 to 300 °C; meanwhile, the intensity of the other weight-loss stage, in the range 300–450 °C, decreased upon increasing the curing temperature. These TGA data suggest that the presence of PVPh in the NDOPda Bz blend had certain advantages: it decreased the temperature for ring opening of the benzoxazine to be below 210 °C, it accelerated the rate of benzoxazole ring formation of NDOPda Bz at a lower temperature (300–450 °C), and it improved the thermal stability of the formed polybenzoxazole.

Fig. 13 presents TGA thermograms of the NDOPda Bz polymer after curing at 300 °C, the NDOPda Bz/PVPh (50/50) blend after curing at 300 °C, and the PVPh. The values of T_{d10} for the NDOPda Bz polymer, the NDOPda Bz/PVPh (50/50) blend, and the PVPh were 460, 461, and 362 °C, respectively;
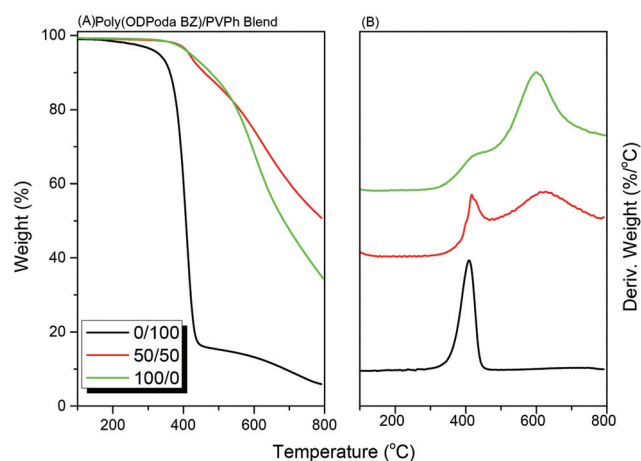

Fig. 13 TGA analyses of the PVPh, the NDOPda Bz/PVPh (50/50) blend, and the NDOPda Bz polymer.

their char yields were 33, 52, and 6%, respectively. Thus, the char yield of the blend was higher than that of the NDOPda Bz polymer itself, suggesting that either (i) strong hydrogen bonding between the NDOPda Bz polymer and the PVPh or (ii) the PVPh homopolymer taking part in the crosslinking reaction with the benzoxazine monomer led to an increased crosslinking density and, thereby, enhanced thermal stability of the NDOPda Bz/PVPh blend system.[11] In addition, as revealed in the derivative weight loss curves, the hydrogen bonding interactions in the blend system accelerated the rate of benzoxazole ring formation of NDOPda Bz at a lower temperature (300 °C).

Conclusions

We have synthesized a new poly(benzoxazine imide), NDOPoda Bz, through a one-pot reaction of naphthalene dianhydride *ortho*-phenol (ND-*ortho*-phenol), paraformaldehyde, and ODA. This poly(benzoxazine imide) was formed without the need to synthesize an amine-functional benzoxazine nor the use of subsequent thermal treatment, as has been the case in previous reports. In addition we converted this poly(benzoxazine imide) into highly cross-linked poly(benzoxazine imide) and highly cross-linked polybenzoxazole through thermal treatment at 240 and 500 °C, respectively. Interestingly, blending of the poly(benzoxazine imide) (NDOPoda Bz) with PVPh, with hydrogen bonding occurring between the C=O groups of NDOPoda BZ and the OH groups of PVPh, had several positive effects: higher glass transition temperatures, char yields, and thermal stability. The presence of hydrogen bonds in the blend had additional attractions: decreasing the temperature for ring opening of the benzoxazine to below 210 °C, accelerating the rate of benzoxazole ring formation of the NDOPda Bz at a lower temperature (300–450 °C), and improving the thermal stability of the formed polybenzoxazole. Therefore, we anticipate that this simple approach might be applicable for preparing super high-performance poly(benzoxazine imide)s.

Conflicts of interest

There are no conflicts to declare.

Acknowledgements

References

1 F. Holly and A. C. Cope, *J. Am. Chem. Soc.*, 1944, **66**, 1875–1879.
2 X. Ning and H. Ishida, *J. Polym. Sci., Part A: Polym. Chem.*, 1994, **32**, 1121–1129.

3 H. Ishida, in *Handbook of Benzoxazine Resins*, ed. H. Ishida and T. Aaga, Elsevier, Amsterdam, 2011, pp. 3–81.

4 P. Froimowicz, L. Han, R. Graf, H. Ishida and C. R. Arza, *Macromolecules*, 2017, **50**, 9249–9256.

5 C. Sawaryan, K. Landfester and A. Taden, *Macromolecules*, 2010, **43**, 8933–8941.

6 Y. X. Wang and H. Ishida, *Polymer*, 1999, **40**, 4563–4570.

7 A. Sudo, R. Kudo, H. Nakayama, K. Arima and T. Endo, *Macromolecules*, 2008, **41**, 9030–9034.

8 X. Li, Y. Xia, W. Xu, Q. Ran and Y. Gu, *Polym. Chem.*, 2012, **3**, 1629–1633.

9 Y. Yagci, B. Kiskan and N. N. Ghosh, *J. Polym. Sci., Part A: Polym. Chem.*, 2009, **47**, 5565–5576.

10 C. F. Wang, Y. C. Su, S. W. Kuo, C. F. Huang, Y. C. Sheen and F. C. Chang, *Angew. Chem., Int. Ed.*, 2006, **45**, 2248–2251.

11 S. W. Kuo, Y. C. Wu, C. F. Wang and K. U. Jeong, *J. Phys. Chem. C*, 2009, **113**, 20666–20673.

12 C. F. Wang, S. F. Chiou, F. H. Ko, J. K. Chen, C. T. Chou, C. F. Huang, S. W. Kuo and F. C. Chang, *Langmuir*, 2007, **23**, 5868–5871.

13 Y. Yagci, B. Kiskan and N. N. Ghosh, *J. Polym. Sci., Part A: Polym. Chem.*, 2008, **47**, 5565–5576.

14 Q. Li and X. Zhong, *Langmuir*, 2011, **27**, 8365–8369.

15 W. H. Hu, K. W. Huang and S. W. Kuo, *Polym. Chem.*, 2012, **3**, 1546–1554.

16 C. F. Wang, S. W. Kuo, C. H. Lin, H. G. Chen, C. S. Liao and P. R. Hung, *RSC Adv.*, 2014, **4**, 36012–36016.

17 C. C. Yang, Y. C. Lin, P. I. Wang, D. J. Liaw and S. W. Kuo, *Polymer*, 2014, **55**, 2044–2050.

18 G. M. Mohamed, K. C. Hsu and S. W. Kuo, *Polym. Chem.*, 2015, **6**, 2423–2433.

19 H. K. Shih, C. C. Hsieh, M. G. Mohamed, C. Y. Zhu and S. W. Kuo, *Soft Matter*, 2016, **12**, 1847–1858.

20 H. K. Fu, C. F. Huang, S. W. Kuo, H. C. Lin, D. R. Yei and F. C. Chang, *Macromol. Rapid Commun.*, 2008, **29**, 1216–1220.

21 H. W. Cui and S. W. Kuo, *J. Polym. Res.*, 2013, **20**, 114.

22 W. H. Hu, K. W. Huang, C. W. Chiou and S. W. Kuo, *Macromolecules*, 2012, **45**, 9020–9028.

23 M. G. Mohamed and S. W. Kuo, *Polymers*, 2016, **8**, 225.

24 Y. T. Liao, Y. C. Lin and S. W. Kuo, *Macromolecules*, 2017, **50**, 5739–5747.

25 T. Agag and T. Takeichi, *Macromolecules*, 2001, **34**, 7257–7263.

26 R. Kudoh, A. Sudo and T. A. Endo, *Macromolecules*, 2010, **43**, 1185–1187.

27 S. Ohashi, J. Kilbane, T. Heyl and H. Ishida, *Macromolecules*, 2015, **48**, 8412–8417.

28 Y. C. Su, S. W. Kuo, D. R. Yei, H. Y. Xu and F. C. Chang, *Polymer*, 2003, **44**, 2187–2191.

29 X. Li, Y. Xia, W. Xu, Q. Ran and Y. Gu, *Polym. Chem.*, 2012, **3**, 1629–1633.

30 H. Ohya, V. V. Kudryavsev and S. I. Semenova, *Polyimide Membranes: Applications, Fabrications and Properties*, Gordon and Breach, Amsterdam, The Netherlands, 1996.

31 K. L. Mittal, *Polyimides: Synthesis, Characterization, and Applications*, Plenum, New York, 1984.

32 P. Vandezande, L. E. M. Gever and I. F. J. Vankelecom, *Chem. Soc. Rev.*, 2008, **37**, 365–405.

33 A. Tiwari, A. K. Nema, C. K. Das and C. K. Nema, *Thermochim. Acta*, 2004, **417**, 133.

34 C. E. Stoog, A. L. Endrey, V. S. Abramo, C. E. Berr, W. M. Edward and K. J. Olivier, *J. Polym. Sci., Part A: Gen. Pap.*, 1965, **3**, 1373–1390.

35 J. Liu and H. Ishida, *Macromolecules*, 2014, **47**, 5682–5690.

36 T. Agag, J. Liu, R. Graf, H. W. Spiess and H. Ishida, *Macromolecules*, 2012, **45**, 8991–8997.

37 M. Minami, T. Endo and S. N. Kolanadiyil, *Macromolecules*, 2017, **50**, 3476–3488.

38 T. J. Dingemans, E. Mendes, J. J. Hinkley, E. S. Weiser and T. L. StClair, *Macromolecules*, 2008, **41**, 2474–2483.

39 K. Zhang, J. Liu and H. Ishida, *Macromolecules*, 2014, **47**, 8674–8681.

40 K. Zhang and H. Ishida, *Polym. Chem.*, 2015, **6**, 2541–2550.

41 K. Zhang and H. Ishida, *Front. Mater.*, 2015, **2**, 5.

42 K. Zhang, J. Qiu, S. Li, Z. Shang and J. Wang, *J. Appl. Polym. Sci.*, 2017, **134**, 45408.

43 M. W. Wang, C. H. Lin and T. Y. Juang, *Macromolecules*, 2013, **46**, 8853–8863.

44 M. Hasegawa and S. Horii, *Polym. J.*, 2007, **39**, 610–621.

45 Y. Gao, F. Y. Q. Huang, Y. Zhou and L. Du, *High Perform. Polym.*, 2013, **25**, 677–684.

46 K. Zhang and H. Ishida, *Polymer*, 2015, **66**, 240–248.

47 K. P. Pramoda, S. L. Liu and T. S. Chung, *Macromol. Mater. Eng.*, 2002, **287**, 931–937.

48 C. L. Lin, W. C. Chen, C. S. Liao, Y. C. Su, C. F. Huang, S. W. Kuo and F. C. Chang, *Macromolecules*, 2005, **38**, 6435–6444.

49 T. K. Kwei, *J. Polym. Sci., Polym. Lett. Ed.*, 1984, **22**, 307–313.

50 J. Y. Wu, M. G. Mohamed and S. W. Kuo, *Polym. Chem.*, 2017, **7**, 5481–5489.